

## FEDSM-ICNMM2010-3085

### THE EFFECT OF DIFFERENT MONOLITHICALLY INTEGRATED CHECK VALVE DESIGNS ON THE EFFICIENCY OF DISPOSABLE PZT-PDMS-MICROPUMPS

**Stefanie Demming**  
IMT, TU Braunschweig  
Braunschweig, Germany

**Ahmed Fadl**  
IMT and IRMB, TU Braunschweig  
Braunschweig, Germany  
ME, University of Rhode Island  
Kingston, RI, USA

**Mareike Schießmann**  
IMT, TU Braunschweig  
Braunschweig, Germany

**Björn Hoxhold**  
IMT, TU Braunschweig  
Braunschweig, Germany

**Zongqin Zhang**  
ME, University of Rhode Island  
Kingston, RI, USA

**Stephanus Büttgenbach**  
IMT, TU Braunschweig  
Braunschweig, Germany

#### ABSTRACT

In the presented study, check valve micropumps with three different valve designs have been developed, fabricated, and successfully tested. These check valves – in the form of differently shaped flaps – were integrated monolithically within the microchannel inlet and outlet of the pump chamber which allows for rapid and inexpensive fabrication of the device. The pump is made of Polydimethylsiloxane (PDMS) with a fully integrated circular piezo-electric transducer (PZT) as a micropump actuator. The performance of the micropumps was characterized under different actuator frequencies, depending on the excitation signal (square, sinusoidal or saw tooth), the implemented PZT diameter (10 mm or 15 mm), as well as the applied offset voltage (positive or negative). Ethanol was used as the working fluid in all experiments. The fabrication technology of the monolithically designed micropump is described, and the results are presented in terms of flow rates. The presented work suggests that the check valve design has an apparent effect on the micropump performance under different operational conditions. All in all, the first results show promising characteristics for easy and inexpensive integration of the proposed micropump in disposable lab-on-a-chip systems.

#### INTRODUCTION

Over the last ten years many research was invested in the development, simulation and optimization of micropumps [1,2]. Despite the different types of micropumps including mechanical and non-mechanical micropumps, check-valve micropumps are one of the most efficient micropumps in terms

of flow rates, maximum back pressure, and self priming capabilities. The challenge of rapid and easy integration of micropumps in disposable lab-on-a-chip systems is to assure simple process technologies based on monolayer structures as these geometries avoid unnecessary dead volumes and ensure flexible implementation. Of course, the easiest way would be the implementation of valve-less geometries, for example based on bifurcation configurations, by change of the channel geometry [3]. However, the obtained flow rates are generally lower when compared to check valve designs. Other attempts have been done by Huang et al. [4] and Yang et al. [5] who reported on planar check valve designs using a movable PDMS-block to open the valve. A more integrative design of the check valve within the pump designs were reported by Adams et al. [6], Yang et al. [7] and Loverich et al. [8]. The implemented valves are based on PDMS flaps fabricated via a double lithographic process.

In this present work, two new designs of planar check valves based on monolithographic processing are presented and compared to the already existing planar flap valves [8].

#### DESIGN

The PZT-PDMS micropump presented here, consists of a monolithically structured PDMS top including the pump chamber, the inlet and outlet channels and the check valves (Figure 1). This PDMS element is covalently bonded to a soda-lime glass, which is preliminarily structured with gold pads at the positions of the check valves.

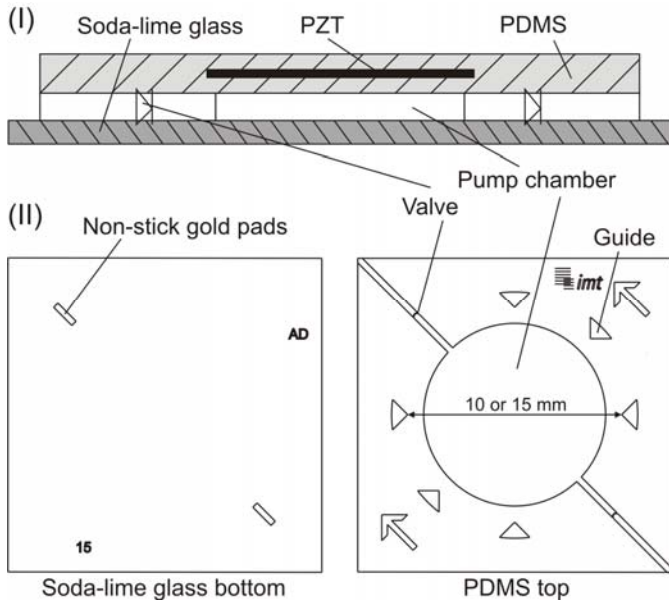


Figure 1: (I) Sectional view of the micropump, (II) top view of the gold structured bottom made of soda-lime glass (left) and the PDMS structured top (right)

The gold pads do not allow for the covalent attachment of the PDMS valves (which feature the same height as the channel due to monolithographic structuring) to the glass bottom during bonding process. This ensures therefore the mobility of the valves during pumping configuration with a minimum leakage gap between the valve and the bottom.

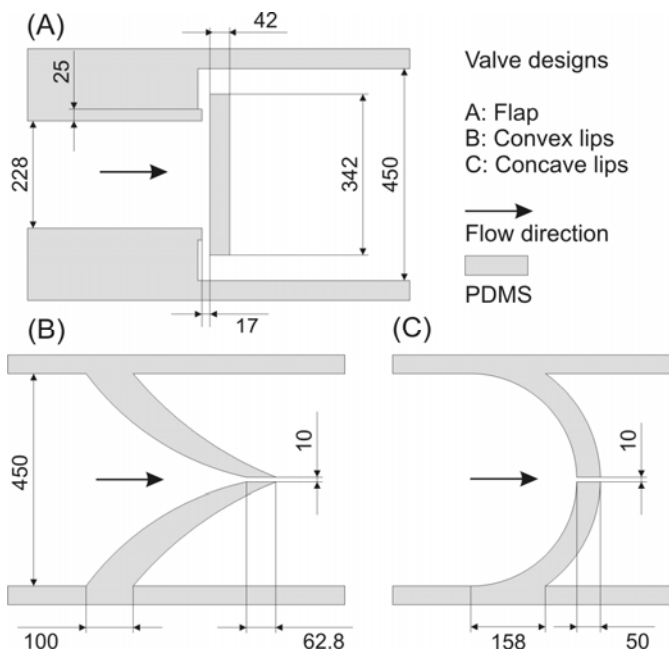


Figure 2: Check valve configurations with dimensions in  $\mu\text{m}$ : (A) flap, (B) convex lips, (C) concave lips

Three different passive check valve designs were developed: a PDMS flap being only fixed to the ceiling of the channel (A), designs based on convex lips (B), or concave lips (C) (Figure 2). The first design (A) is similar to the configuration already presented in [8], whereas designs (B) and (C) are presented - to the best of our knowledge - for the first time in literature. The lips of (B) and (C) are fixed on two axes to the PDMS: to the ceiling as well as to the wall of the microchannel. Two mirrored lips within one channel are separated from each other via a  $10\ \mu\text{m}$  air gap. For all three valve designs two different diameters of the pump chamber were tested:  $8.5\ \text{mm}$  diameter for the  $10\ \text{mm}$  diameter PZT and  $12.75\ \text{mm}$  for the  $15\ \text{mm}$  diameter PZT. The channel height of the pump is  $230\ \mu\text{m}$ . The guides around the pump chamber (Figure 1 (II), right) were implemented in the mask design in order to better align the PZT actuators during the fabrication process.

## FABRICATION

### Structured PDMS top

The structured PDMS top including channels, pump chamber, guides and valves is fabricated via softlithographic processing and PDMS replica molding. A  $700\ \mu\text{m}$  thick soda-lime glass is used as substrate for the SU-8 negative master. After cleaning and dehydration (1 h at  $120\ ^\circ\text{C}$ ), the substrate is activated with oxygen plasma (plasma activate flecto 10USB, Plasma Technology, Germany). Directly after, the first SU-8 layer (SU-8 5 from MicroChem, Corp., Newton, MA, USA) is spun on at  $3000\ \text{rpm}$  for 30 s and dried for 10 min at  $95\ ^\circ\text{C}$ . This layer - acting both as an adhesion promoter and seed layer for the following structure SU-8 layer - is flood exposed to UV-light and baked at  $95\ ^\circ\text{C}$  for 10 min. Before spin coating of the structure layer the seed layer is activated in oxygen plasma. SU-8 50 is applied at  $1200\ \text{rpm}$ , leveled and dried at  $95\ ^\circ\text{C}$  for 2 h. The same process step is repeated - including an additional hour of drying - in order to attain a total layer thickness of  $230\ \mu\text{m}$ . Then, the substrate is exposed to UV-light for 100 s. A post exposure bake follows for 20 min at  $95\ ^\circ\text{C}$ . The fabrication of the negative master concludes with the development in propylene glycol methyl ether acetate (PGMEA, MicroChem Corporation, Newton, MA, USA). Replica of this master is done by using PDMS (Sylgard 184 elastomer kit, Dow Corning, Midland, MI, USA) in the standard ratio of 10:1 (silicon elastomer base : curing agent). A defined PDMS membrane thickness of  $200\ \mu\text{m}$  is produced via the double sided molding device [9] guaranteeing that the membrane thicknesses of all micropumps are identical. After degassing, the PDMS is heated at  $80\ ^\circ\text{C}$  for 30 min, peeled off from the master and cut into single pieces.

### Gold structured glass bottom

A soda-lime glass ( $700\ \mu\text{m}$ ) is also employed for the gold structured glass bottom. After cleaning, the wafer is dehydrated at  $120\ ^\circ\text{C}$  for 1 h. Secondly, a chromium-gold layer ( $10\ \text{nm}$  and

275 nm, respectively) is sputtered on the cleaned side and spin-coated with positive resist ma-P 1215 (micro resist technology GmbH, Berlin, Germany). After a softbake of 1 min, the resist is exposed to UV-light for 10 s and finally developed in ma-D 331 (micro resist technology GmbH, Berlin, Germany). Before the etching of the gold and chromium, the wafer is hydrophilized with oxygen plasma. After the etching process, the wafer is diced into the single elements which are then cleaned by use of acetone and ethanol.

### Assembling of the micropump

The PDMS top elements are covalently bonded via oxygen plasma activation to the corresponding glass bottoms. The flexibility in alignment of both top and bottom element is given by the use of ethanol which prolongs the time of surface activation. Another plasma treatment follows to activate the top side of the PDMS. The PZT actuator, which was preliminary connected with wire, is centrally aligned on top of the surface activated PDMS according to the guides. Then fresh PDMS is poured on top of the system and dried at 70 °C for again 1 h. The fixation of the PZT to the PDMS can even be ameliorated by the use of silicone glue (RS 692-542, RS Components Ltd., UK) applied between PDMS membrane and the PZT. Finally, the assembled micropump is connected with inlet and outlet metallic micropipes (outer diameter 0.55 mm) (Sterican, B. Braun, Germany) and the pump is ready for use (Figure 3).

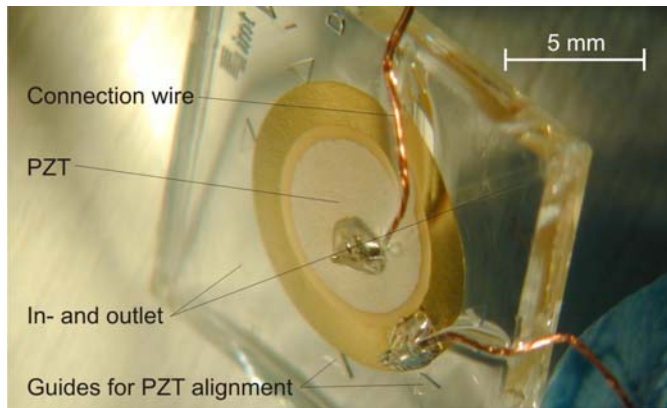


Figure 3: Photo of the assembled PZT-PDMS-micropump

### CHARACTERIZATION

Figure 4 illustrates the experimental apparatus used for the characterization of the different micropumps. The set-up consists of a frequency generator (Agilent 33220A, Agilent Technologies GmbH, Böblingen, Germany), an amplifier (E-508.00 HVPZT, PI Physik Instrumente, Karlsruhe, Germany) set to excite a constant voltage of 200 V<sub>pp</sub> and an oscilloscope (Tektronix, Japan). Moreover, the flow in real time within the micropump can be monitored via a digital microscopic camera (dnt GmbH, Dietzenbach, Germany) which is directly connected to a computer.

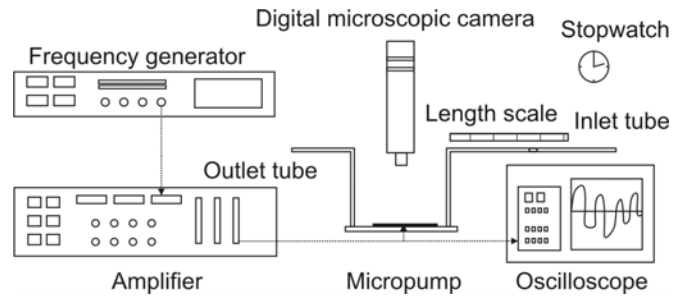


Figure 4: Experimental set-up used for the characterization of the PZT-PDMS micropump

To evaluate the pump efficiencies of the different check valve designs for different conditions, the flow rate was measured by means of the bubble tracking method described in [10]. An air bubble is trapped in the inlet tube and the time in which the air bubble requires to move a defined distance (5 cm and 10 cm) is recorded. According to this measurement procedure, the flow rates are analyzed for the three valve designs. Moreover, the dependency on the excitation frequency, the signal (square, sinusoidal or saw tooth), the PZT diameter and the offset voltage is characterized and discussed in the following. Ethanol was used as the working fluid in all experiments; however the use of de-ionized water was also tested – as it is usually used for lab-on-a-chip applications – and showed a decrease of the flow rate to one third of the flow rate obtained with ethanol. It has to be considered, that the use of ethanol might modify the mechanical properties of the PDMS valves, since it slightly swells as reported in [11] according to a swelling ratio of 1.04. This is avoided by the use of water.

### Comparison of the different check valves

Figure 5 depicts the flow rates in conjunction with the excitation frequency for the check valve designs A, B and C with a PZT of 15 mm in diameter.

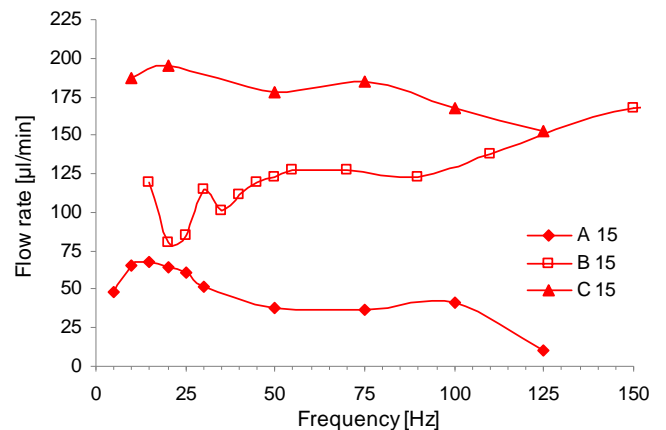


Figure 5: Pump rate versus frequency (0-150 Hz) for the three different check valve designs (A, B and C) and a PZT diameter of 15 mm using a square signal

It is clearly noticeable that valve design C (concave lips) achieves best pumping rates for the low frequency range, slightly decreasing for increasing frequencies. For design B a different characteristic can be noticed. It displays only half as much of the pump rate values obtained with design C at very low frequencies, but then shows increasing performance for augmenting excitation frequencies. Design A (flap design) is associated with the lowest pumping capability for the entire analyzed frequency range. This could be due to the leakage gaps – and thus the increased losses – in two axes when compared to the lip design which reveals an open gap in only one axis. Moreover, the lower pump performance of design C might result from the channel restriction before the valve flap.

### Variation of excitation signal

Since the micropump design with the overall highest flow rate resulted to be the one with concave lips (design C), this design was then used for characterization of the dependency on the signal variation: square, sinusoidal or saw tooth. Figure 6 demonstrates the flow rate curves versus the excitation frequency for the three different signals. The used micropump is design C 15 with an implemented PZT of 15 mm in diameter.

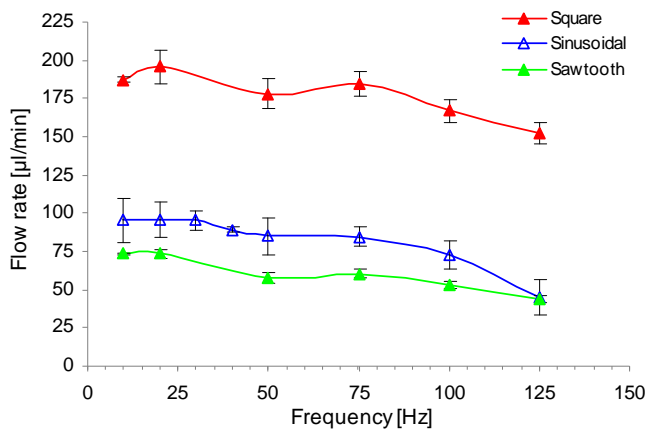


Figure 6: Flow rate versus frequency for different input signals (square, sinusoidal, saw tooth) with micropump C 15 (PZT diameter of 15 mm)

The standard deviation of the different curves is based on 2-8 measurements with the square signal, 2-6 with the sinusoidal signal and 2-4 with saw tooth excitation frequency. It can clearly be seen that by use of a square signal the flow rate is significantly – two to three times – higher (between 150 and 200 µL/min) than the pump rate obtained with a sinusoidal or saw tooth wave (between 50 and 100 µL/min). The latter signal produces even smaller pumping values than the sinusoidal one. This result is in accordance with the

measurements done by Forster et al. [12] who reported higher flow rates for square signals than for sinusoidal waves.

### Variation of PZT diameter

Experimental results in Figure 7 illustrate the flow rates versus frequency for different excitation voltages, again using valve design C. However, the difference compared to Figure 6 is the use of a micropump with a PZT diameter of 10 mm instead of 15 mm. The standard deviations were again calculated for 2 to 8 tests run under same conditions. It is striking that the characteristic curves for both pump sizes are quite similar to each other. Yet again best pump performance results by the use of a square wave signal. Not only are the profiles of the curves alike but also the values of the pump rates.

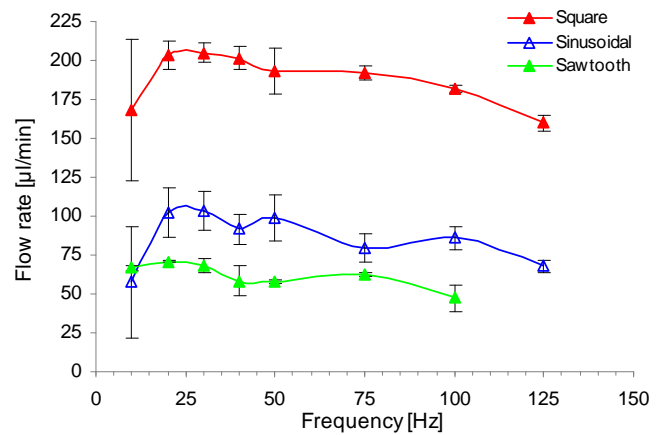


Figure 7: Flow rate versus frequency for different input signals (square, sinusoidal, saw tooth) with micropump C 10 (PZT diameter of 10 mm).

Generally said, a better performance should be presumed for a bigger PZT, since the compression rate (ratio of the displaced volume to the dead volume) should be higher for larger PZT actuators. Only one difference in the fabrication procedure was done for the pump design C 10, where a silicone rubber sealing was added between the PDMS membrane and the PZT. This could have ensured a better fixation of the oscillating PDMS membrane to the PZT. Therefore, further analysis of two new micropumps is necessary in order to confirm or disprove the statement of equal pumping performance for 10 and 15 mm PZT diameters. The maximum back pressure of 2.3 kPa was obtained for the C 10 design.

### Variation of offset voltage

By oscillating a given frequency not around zero, but with a positive or negative offset, a change in flow rate can be obtained. As illustrated in Figure 8, a vivid increase in flow rate was achieved when increasing the offset from zero to +50 V. For both designs A 10 and B 10, a linear correlation (measured

for three fixed offset voltages) could be detected, resulting in a flow rate of 422  $\mu\text{L}/\text{min}$  with a positive offset of 50 V for design A 10 at a frequency of 50 Hz. This reflects a 10 times higher flow rate when compared to pumping without an offset. Micropump B 10 shows similar behavior.

However, when applying a positive offset voltage to the micropump C 10 a small decrease in flow rate was detected. For negative offset voltages of -10 V and -50 V, the flow rate augmented almost linearly from 107  $\mu\text{L}/\text{min}$  to 181  $\mu\text{L}/\text{min}$ , respectively.

The first results obtained for the variation of offset voltage are contradictory and need more investigation. However, one result is certain: the used offset voltage has a significant effect on the pumping performance.

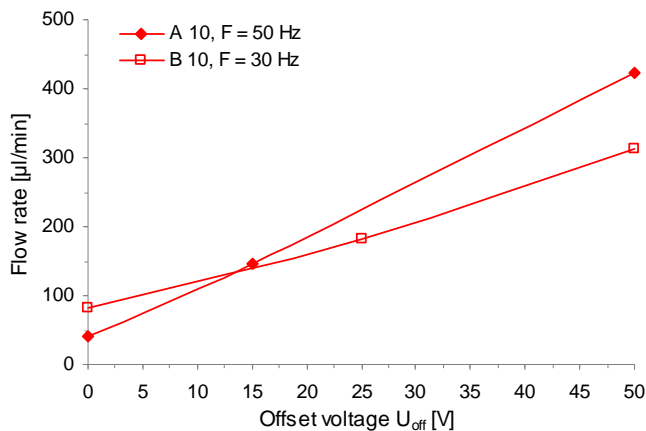


Figure 8: Flow rate in dependence on the offset voltage for the micropumps A 10 and B 10 with a square wave frequency of 50 Hz and 30 Hz, respectively

## CONCLUSION

Three different self-priming micropumps based on monolithically structured PDMS check valves ((A) flap, (B) convex lips and (C) concave lips) were developed, fabricated, and successfully characterized. By the use of structured glass bottoms with non-stick gold pads, the mobility of the valve flaps/lips can be guaranteed with minimum leakage gap.

In the first experiments the pump design C was associated with the highest resulting flow rates of almost 200  $\mu\text{L}/\text{min}$  (voltage of 200  $V_{\text{pp}}$  and no offset), followed by design B. The lowest pump rate was obtained with the flap design A. Moreover, a significant effect of the set input signal (square, sinusoidal, tooth saw) on the pump performance exists. The square wave signal was always associated with the best pumping capabilities. When comparing two different sizes of used PZTs (15 mm and 10 mm), no remarkable differences in pumping rates could be detected. The only difference was – besides the diameter of the PZT – that the micropump with 10 mm PZT featured a silicone rubber sealing between PZT and the PDMS membrane in addition to the standard fabrication process. It has still not been verified whether this

change in fabrication creates large differences in pumping performance. Last but not least, a remarkable dependency of the flow rate on the set positive or negative offset voltage could be encountered. Yet before making specific conclusions on any dependencies, more tests should be conducted.

In summary, the presented check valve based micropump reveals high potential of easy and inexpensive integration in monolithically fabricated, disposable lab-on-a-chip systems.

## ACKNOWLEDGMENTS

The authors thank the German Research Foundation (DFG) for support of this work in the framework of the Collaborative Research Group mikroPART (Micro systems for particulate life-science products).

## REFERENCES

- [1] N. Nguyen, X. Huang, T. K. Chuan (2002), MEMS-micropumps: a review, *J Fluid Eng* 124, 384-392
- [2] F. Amirouch, Y. Zhou, T. Johnson (2009), Current micropump technologies and their biomedical applications, *Microsyst Technol* 15, 647-666
- [3] A. Fadl, S. Demming, Z. Zhang, S. Büttgenbach, M. Krafczyk, D. M. L. Meyer (2009), A multifunction and bidirectional valve-less rectification micropump based on bifurcation geometry, *Microfluid Nanofluid*, DOI: 10.1007/s10404-009-0544-0, 1-14
- [4] C. J. Huang, G. B. Lee (2007), A microfluidic system for automatic cell culture, *J Micromech Microeng* 17, 1266-1274
- [5] Y. N. Yuang, S. K. Hsiung, G. B. Lee (2009), A pneumatic micropump incorporated with a normally closed valve capable of generating a high pumping rate and a high back pressure, *Microfluid Nanofluid* 6, 823-833
- [6] M. L. Adams, M. L. Johnston, A. Scherer, S. R. Quake (2005), Polydimethylsiloxane based microfluidic diode, *J Micromech Microeng* 15, 1517-1521
- [7] B. Yang, Q. Lin (2007), Planar micro-check valves exploiting large polymer compliance, *Sensors Actuators A* 134, 186-193
- [8] J. J. Loverich, I. Kanno, H. Kotera (2007), Single-step replicable microfluidic check valve for rectifying and sensing low Reynolds number flow, *Microfluid Nanofluid* 3, 427-435
- [9] N. Lucas, S. Demming, A. Jordan, P. Sichler, S. Büttgenbach (2008), An improved method for double-sided moulding of PDMS, *J Micromech Microeng* 18, 075037
- [10] J. Yoon, J. Choi, H. Lee, M. Kim (2007), A valveless micropump for bidirectional applications, *Sensors Actuators A* 135, 833-838
- [11] J. Ng Lee, C. Park, G. M. Whitesides (2003), Solvent Compatibility of Poly(dimethylsiloxane)-Based Microfluidic Devices, *Anal Chem*, 75, 6544-6554
- [12] F. K. Forster, L. Bardell, M. A. Afromowitz, N. R. Sharma, A. Blanchard (1995), Design, fabrication and testing of fixed-valve micro-pumps, *Proc ASME Fluids Eng Div ASME* 234, 39-44